

Does Planck really rule out monomial inflation?

Kari Enqvist and Mindaugas Karčiauskas

Physics Department and Helsinki Institute of Physics

PO Box 64, FIN-00014 University of Helsinki

Abstract

We consider the modifications of monomial chaotic inflation models due to radiative corrections induced by inflaton couplings to bosons and/or fermions necessary for reheating. To the lowest order, ignoring gravitational corrections and treating the inflaton as a classical background field, they are of the Coleman-Weinberg type and parametrized by the renormalization scale μ . In cosmology, there are not enough measurements to fix μ so that we end up with a family of models, each having a slightly different slope of the potential. We demonstrate by explicit calculation that within the family of chaotic ϕ^2 models, some may be ruled out by Planck whereas some remain perfectly viable. In contrast, radiative corrections do not seem to help chaotic ϕ^4 models to meet the Planck constraints.

I. INTRODUCTION

Planck data has famously been used to constrain single-field inflaton models, such as large-field models with a monomial potential $V \sim \phi^n$. Such models can be considered as effective particle physics theories with heavy degrees of freedom and/or interactions with other fields integrated out. From such a point of view one may justify e.g. neglecting the running of λ in $\lambda\phi^4$ model and treat it as an effective constant. Adopting such an approach, Planck rules out chaotic $\lambda\phi^4$ models while $m^2\phi^2$ models may still be allowed, albeit marginally.

However, we should like to point out that inflaton decay is an essential part of any inflationary scenario that cannot be integrated out. Thus, any model must be augmented by a mechanism that brings inflation to an end and reheats the universe. As is well known, this means adding interaction terms to a model so that to lowest order the potential in monomial inflation would read like

$$V(\phi, \chi, \psi) = \frac{1}{2}\lambda_b m_{\text{Pl}}^4 \left(\frac{\phi}{m_{\text{Pl}}}\right)^n - \frac{1}{2}g_b^2 \phi^2 \chi^2 - h_b \phi \bar{\psi} \psi + \dots \quad (1)$$

where χ is some bosonic and ψ fermionic field, and the subscript ‘b’ denotes bare coupling constant values. Dots represent other terms, such as mass terms for the fields χ and ψ . These interactions will then generate through loop corrections operators that modify the effective inflaton potential. Here we focus on the minimal modifications only. We take χ and ψ to be quantum fields while the inflaton ϕ is treated as a classical background field. In particular, this means neglecting the inflaton loops. Moreover, we do not consider quantum corrections in curved space background, which can induce additional curvature-dependent terms [1] into the potential (1). The issue with the curved space corrections is not just the vacuum structure but there may also arise corrections to the slow-roll equations of the mean field [2]. To circumvent these complications, and for the sake of clarity, we view the first term in (1) as the effective energy of an order parameter that is the source of the Friedmann equation after integrating out the additional gravitational effects.

To lowest order the modifications are then of the conventional Coleman-Weinberg type. The properly regulated effective inflaton model would thus read

$$V_{\text{eff}}(\phi) = \frac{1}{2}\lambda m_{\text{Pl}}^4 \left(\frac{\phi}{m_{\text{Pl}}}\right)^n + \frac{g^4 - 4h^4}{64\pi^2} \phi^4 \ln \frac{\phi^2}{\mu^2}, \quad (2)$$

where g and h are renormalized coupling constants, and by virtue of the classical nature of ϕ , $\lambda = \lambda_b$. Renormalizability requires $n \leq 4$ and we have assumed $g\phi \gg m_\chi$ and $h\phi \gg m_\psi$, where m_χ and m_ψ are masses of χ and ψ fields respectively and these terms are included in the part of the potential denoted by ellipsis in Eq. (1). For self-consistency of the model, radiative corrections to the potential must be taken into account when estimating the number of e-folds and values of the slow-roll parameters. This is the purpose of the present paper.

The importance of radiative corrections for chaotic inflation was already pointed out by Senoguz and Shafi in [3]. They considered only fermionic contributions, but more importantly, they chose the renormalization scale as $\mu = hM_P$. The renormalization scale is of course arbitrary; there is no "natural" scale μ except in the technical sense of minimizing higher order corrections. In particle physics, one trades μ with a measured value of some physical amplitude; this is the act of "normalization". For instance, one could measure a $2 \rightarrow 2$ scattering amplitude at some fixed external momenta \mathbf{p} (and most conveniently at the symmetric point with all the momenta equal) to extract the coupling constant at the renormalization point $p^2 = \mu^2$. After that, the truncated perturbative expression yields the running of the amplitude (or coupling) as the response to the scaling of the external momenta. For inflationary models, the situation is trickier. For instance, the physical inflaton mass could be defined as the pole mass $m_{\text{phys}} = m(p^2 = m_{\text{phys}}^2)$, where m is the bare mass, which is a parameter in the potential. Unfortunately, there are no prospects for measuring the physical inflaton mass independently of cosmological observations. Thus the question is, what exactly is the meaning of the potential parameters that can be constrained by CMB observations - and which models are truly ruled out?

As far as the Planck constraints are concerned, we shall point out that different renormalization points correspond to physically different models of inflation in that they lead to different predictions for the observables n_s and r . The models are different in the sense that the shape of the potential at some fixed ϕ is different for different renormalization points; likewise, given identical initial conditions, they would yield a different number of e-folds. Alternatively, by fixing, say, the value of the spectral index, one would obtain a family of models with the same n_s but with different physical model parameters m (or λ) and g or h . As we shall show, for the ϕ^2 potential some of the models in this family are ruled out while some remain perfectly viable. We should emphasize that we consider only cases where

the radiative corrections are always small. For the ϕ^4 potential this restricts the possible modifications so that this class of models is always ruled out by the Planck data.

Here we differ from the approach of Senoguz and Shafi [3] who fix the renormalization point and claim that the fixing does not affect physics. This is of course true in the sense that observables, such as scattering cross sections, are not affected. However, cosmological constraints on model parameters – which are not observables – very much depend on at which scale those parameters are being defined.

II. PLANCK CONSTRAINTS ON LARGE-FIELD MONOMIAL INFLATION

Let us provide a brief summary of the relevant Planck results and constraints. In single field inflation models the value of the energy density at every space-time position (\mathbf{x}, t) is determined completely by the value of the inflaton field $\phi(\mathbf{x}, t)$. Hence, $\phi(\mathbf{x}, t)$ also determines the time shift between the flat and uniform energy density hypersurfaces, where the perturbation spectrum is being computed. It is given by [4]

$$\mathcal{P}_\zeta(k) = \frac{1}{24\pi^2 m_{\text{Pl}}^4} \left. \frac{V(\phi)}{\epsilon} \right|_k. \quad (3)$$

The perturbation amplitude $\mathcal{P}_\zeta(k_*)$ at the the pivot scale $k_* = 0.05 \text{ Mpc}^{-1}$ is measured by Planck as [5]

$$\mathcal{P}_\zeta(k_*) = 2.20 \times 10^{-9}. \quad (4)$$

Large-field monomial inflaton models are slow-roll models. The spectral index is given as usual by

$$n_s - 1 = -6\epsilon + 2\eta, \quad (5)$$

and the running of the spectral index

$$n' \equiv \text{d}n_s/\text{d}\ln k = -24\epsilon^2 + 16\epsilon\eta - 2\xi, \quad (6)$$

where slow-roll parameters are defined as

$$\epsilon \equiv \frac{m_{\text{Pl}}^2}{2} \left(\frac{V'}{V} \right)^2, \quad \eta \equiv m_{\text{Pl}}^2 \frac{V''}{V}, \quad \xi \equiv m_{\text{Pl}}^4 \frac{V'V'''}{V^2}, \quad (7)$$

and $V \equiv V(\phi)$ is the potential of the inflaton. Primes denote derivatives with respect to ϕ . During inflation all slow-roll parameters are small, $\epsilon, \eta, \xi \ll 1$.

Tensor-to-scalar ratio obeys the relation

$$r = 16\epsilon. \quad (8)$$

Hence, measuring primordial gravitational waves would allow a direct determination of the energy scale of inflation from Eqs. (3) and (4).

Currently measured value of n_s is [6] (assuming no running and tensor modes)

$$n_s = 0.9603 \pm 0.0073. \quad (9)$$

Allowing for spectral running Planck constraints give

$$n_s = 0.9630 \pm 0.0065, \quad (10)$$

$$n' = -0.013 \pm 0.009 \quad (11)$$

at 68% CL at the decorrelation pivot scale $k_*^{\text{dec}} = 0.038 \text{ Mpc}^{-1}$. As noted in Ref. [6] the value of ξ derived from this measurement is still compatible with zero at 95% CL.

The contamination of the primordial B-mode spectrum mainly by the gravitational lensing signal sets the lowest bound on the value of r which one might hope to ever achieve if not detected. This limit is 10^{-4} or so [7]. There is, however, a class of inflationary models which produce larger r than this limit. Indeed, as emphasized in the Introduction, current observational bounds on r decreased to the level where it becomes possible to falsify some of these models. The most stringent constraints on r are derived from the recent Planck satellite results [6]

$$n_s = 0.9624 \pm 0.0075 \quad (12)$$

$$r < 0.12 \quad (13)$$

at 95% CL and at a pivot scale $k_* = 0.002 \text{ Mpc}^{-1}$.

The Planck team used these results to constrain some of the inflationary models in Ref. [6]. Assuming a simple tree-level potential corresponding to the first term of Eq. (1), they showed that such a low value of r is incompatible with large-field models with a monomial potential $\sim \phi^n$, where $n = 3$ and 4 and only marginally compatible with the $n = 2$ model. They also constrained the linear model as well as a model with $n = 2/3$, both of which are not amenable to conventional perturbation theory. We do not consider such models here.

III. THE EFFECT OF RADIATIVE CORRECTIONS

A. Chaotic Inflation with Radiative Corrections

To simplify the expressions let us rewrite the inflaton potential in Eq. (2) as

$$V_{\text{eff}}(\phi) = \frac{1}{2}\lambda m_{\text{Pl}}^4 \left(\varphi^n + \kappa \varphi^4 \ln \frac{\varphi}{\mu} \right), \quad (14)$$

where φ and κ are defined as

$$\varphi \equiv \frac{\phi}{m_{\text{Pl}}} \quad (15)$$

and

$$\kappa \equiv \frac{g^4 - 4h^4}{16\pi^2\lambda}. \quad (16)$$

In this expression the renormalization scale μ is given in units of the Planck mass. One can immediately notice that the potential can become unbounded from below when the second term in Eq. (14) is negative and dominates. In this regime, however, higher order loop corrections become important and should be included in Eq. (14). As we mainly constrain ourselves within the regime of small radiative corrections, this apparent instability does not have to concern us.

Looking at Eq. (14) it should be clear that radiative corrections change both the slope and the curvature of the potential. Due to Eqs. (5), (6) and (8) observables of CMB, such as the spectral index n_s , its running n' , and tensor-to-scalar ratio r are also modified from their tree level values. Using Eq. (7) one can easily compute the radiatively corrected slow-roll parameters as

$$\epsilon = \frac{K(\varphi)^2}{2\varphi^2} \left[n + \kappa \varphi^{4-n} \left(1 + 4 \ln \frac{\varphi}{\mu} \right) \right]^2, \quad (17)$$

$$\eta = \frac{K(\varphi)}{\varphi^2} \left[n(n-1) + \kappa \varphi^{4-n} \left(7 + 12 \ln \frac{\varphi}{\mu} \right) \right], \quad (18)$$

$$\xi = \frac{K(\varphi)^2}{\varphi^4} \left[n + \kappa \varphi^{4-n} \left(1 + 4 \ln \frac{\varphi}{\mu} \right) \right] \left[n(n-1)(n-2) + \kappa \varphi^{4-n} \left(14 + 46 \ln \frac{\varphi}{\mu} \right) \right] \quad (19)$$

where for brevity we defined

$$K^{-1}(\varphi) \equiv 1 + \kappa \varphi^{4-n} \ln \frac{\varphi}{\mu}. \quad (20)$$

Knowing the values of these parameters a couple of e-folds after the pivot scale k_* exits the horizon, it is easy to compute $n_s(n, \kappa, \mu)$, $n'(n, \kappa, \mu)$ and $r(n, \kappa, \mu)$ using Eqs. (5), (6) and (8) respectively. However, in contrast to the tree level potential, the values of these parameters are determined not only by the power n but also by the strength of the couplings of the inflaton to other fields κ , as well as by the renormalization scale μ .

To find numerical values of slow-roll parameters in Eqs. (17) - (19) we need to solve the system of three coupled equations. The first equation is given by the end of inflation condition. Inflation terminates when the slow-roll parameter ϵ becomes of order one. Hence, we define the inflaton value at the end of inflation φ_{end} as

$$\epsilon(\varphi_{\text{end}}, n, \kappa, \mu) = 1. \quad (21)$$

The number of e-folds of inflation from the time when a mode k leaves the horizon to the end of inflation is given by $N_k \equiv \int_{t_k}^{t_{\text{end}}} H dt = m_{\text{Pl}}^{-2} \int_{\varphi_{\text{end}}}^{\varphi_k} V/V' d\varphi$, where we used the slow-roll result $3H\dot{\varphi} \simeq -V'$. Plugging Eq. (7) into this result we can write for the pivot scale k_*

$$\int_{\varphi_*}^{\varphi_{\text{end}}} \frac{d\varphi}{\sqrt{2\epsilon(\varphi, n, \kappa, \mu)}} = -N_*, \quad (22)$$

where $N_* \equiv N_{k_*}$. One also has to make sure that the solution gives the curvature perturbation amplitude in Eq. (3) consistent with the observed value in Eq. (4). This provides a third equation to compute the (renormalised) inflaton self-coupling constant λ in Eq. (14)

$$\lambda = 24\pi^2 \mathcal{P}_* \frac{\left[n + \kappa \varphi_*^{4-n} \left(1 + 4 \ln \frac{\varphi_*}{\mu} \right) \right]^2}{\varphi_*^{2+n} \left[1 + \kappa \varphi_*^{4-n} \ln \frac{\varphi_*}{\mu} \right]^3}. \quad (23)$$

The value of N_* in Eq. (22) depends on the temperature of reheating $T_{\text{reh}} \propto \rho_{\text{reh}}^{1/4}$ and is given by [8]

$$N_* = 68.5 + \frac{1}{2} \ln \frac{V_*}{m_{\text{Pl}}^4} - \frac{1}{3} \ln \frac{V_{\text{end}}}{m_{\text{Pl}}^4} + \frac{1}{12} \ln \frac{\rho_{\text{reh}}}{m_{\text{Pl}}^4}, \quad (24)$$

where $V_* \equiv V_{\text{eff}}(\phi_*)$, $V_{\text{end}} \equiv V_{\text{eff}}(\phi_{\text{end}})$ and we also used the value of the present day Hubble constant $H_0 = 67.04 \text{ km/s/Mpc}$ [5]. We assume in this work that the inflaton decays through a process of perturbative decay. As N_* depends only on the temperature of reheating, non-perturbative effects will not in general change the results much. In some cases, however, these effects could change the thermal history of the universe [9]. Such cases should be treated separately. For the perturbative decay, on the other hand, we can write

$$\rho_{\text{reh}} \simeq 3m_{\text{Pl}}^2 \Gamma^2, \quad (25)$$

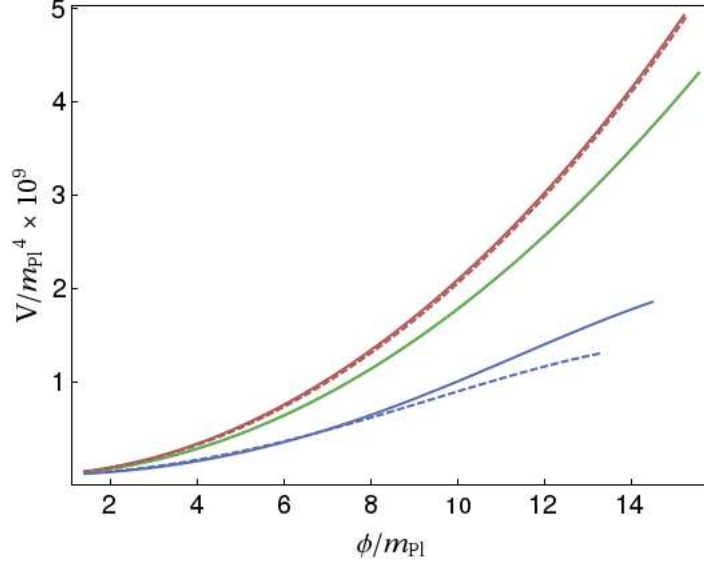


Figure 1. Inflationary parts of $m^2\phi^2$ potentials. The middle, solid green curve correspond to the potential with $N_* = 60$ and $\kappa = 0$ (denoted by the large black dot in Figure 2). Lower blue curves correspond to inflaton potentials denoted by number 1 in Figure 2, while top red curves correspond to number 6 in that Figure.

where Γ is the decay rate of the inflaton.

Scalar spectral index n_s , spectral running n' and tensor-to-scalar ratio r can be calculated by solving Eqs. (21) - (23) for φ_* and plugging the result into Eqs. (5), (6) and (8). Unfortunately it is impossible to solve them analytically. Therefore, one has to resort to numerical methods. As we scan over different values of κ to find solutions of Eqs. (21) - (23), we must also make sure that the universe reheats well before the start of Big Bang Nucleosynthesis, which happens at $T_{\text{BBN}} \sim 1$ MeV. Thus the minimum value of $|\kappa|$ must be constrained to give $T_{\text{reh}} \sim \sqrt{m_{\text{Pl}}\Gamma} > T_{\text{BBN}}$. This bound however, is many orders of magnitude below the values of interest for this work.

B. The Case of $n = 2$

For the quadratic monomial potential with $n = 2$ we can write

$$\lambda = \frac{m^2}{m_{\text{Pl}}^2}, \quad (26)$$

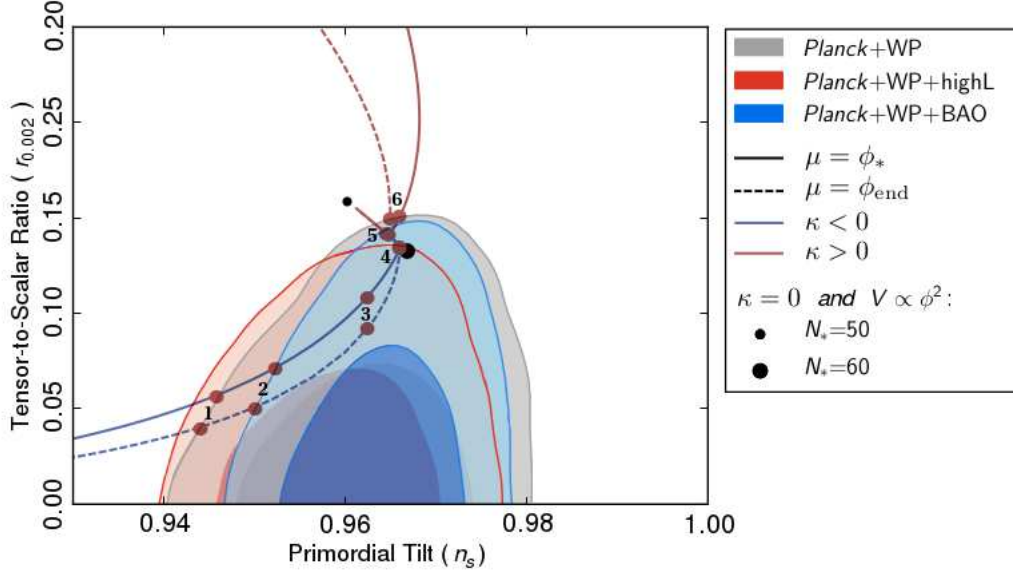


Figure 2. Planck constraints on the spectral index n_s and tensor-to-scalar ratio r [6]. Black dots correspond to the ϕ^2 model with $\kappa = 0$. Solid and dashed curves correspond to normalization scales $\mu = \phi_*$ and $\mu = \phi_{\text{end}}$ respectively. Blue curves show the effect of radiative corrections when the $\phi \rightarrow \bar{\psi}\psi$ decay channel dominates ($\kappa < 0$) and red curves when the $\phi \rightarrow \chi\chi$ channel dominates ($\kappa > 0$). The values of parameters in Table I are denoted by numbers.

where m^2 is the *renormalised* mass of the inflaton. The inflaton decay rate to bosons $\phi \rightarrow \chi\chi$ is given by

$$\Gamma_\chi = \frac{g^4 \sigma^2}{8\pi m}, \quad (27)$$

where σ is the inflaton vacuum expectation value. We assume $\sigma \sim m$ for simplicity. Since N_* depends only logarithmically on σ , the change of the latter will not have a major effect. While the decay rate to fermions $\phi \rightarrow \psi\bar{\psi}$ is given by

$$\Gamma_\psi = \frac{h^2 m}{8\pi}. \quad (28)$$

The total decay rate of the inflaton is a sum of the two $\Gamma = \Gamma_\chi + \Gamma_\psi$. However, we consider only the cases when either Γ_χ or Γ_ψ dominates.

We solve Eqs. (21) - (23) for two choices of renormalization scale μ . In the first case μ is such that radiative corrections vanish when the pivot scale exits the horizon, i.e. $\mu = \phi_*$. In effect, this then corresponds to a "pure" $m^2\phi^2$ model valid at the pivot scale only. The other extreme is the case with $\mu = \phi_{\text{end}}$, where the "pure" $m^2\phi^2$ model is valid at the end

$\mu = \phi_*$							
	1	2	3	4		5	6
κ	-3.7×10^{-3}	-2.8×10^{-3}	-1.0×10^{-3}	-2.0×10^{-5}	0	3.0×10^{-5}	4.0×10^{-4}
n_s	0.9459	0.9524	0.9625	0.9661	0.9670	0.9645	0.9661
r	0.0570	0.0716	0.1089	0.1349	0.132	0.1417	0.1513
$n' \times 10^4$	-6.345	-7.197	-7.122	-5.774	-5.464	-6.140	-5.166
$h, g \times 10^3$	1.268	1.242	1.050	0.414	0	0.662	1.280
$m(10^{13} \text{ GeV})$	1.009	1.113	1.332	1.464	1.01	1.530	1.566
ϕ_*/m_{Pl}	14.49	14.72	15.17	15.37	15.56	15.08	15.22
N_*	58.67	58.73	58.81	58.56	60	56.23	56.74

$\mu = \phi_{\text{end}}$							
	1	2	3	4		5	6
κ	-7.5×10^{-4}	-6.4×10^{-4}	-3.0×10^{-4}	-2.0×10^{-6}	0	8.0×10^{-6}	7.0×10^{-5}
n_s	0.9441	0.9501	0.9626	0.9660	0.9670	0.9647	0.9650
r	0.0403	0.0509	0.0926	0.1356	0.132	0.1425	0.1503
$n' \times 10^4$	3.627	1.876	-2.977	-5.757	-5.464	-6.308	-6.630
$h, g \times 10^4$	8.885	8.856	7.918	2.334	0	4.764	8.182
$m(10^{13} \text{ GeV})$	1.101	1.184	1.383	1.471	1.01	1.533	1.528
ϕ_*/m_{Pl}	13.36	13.67	14.62	15.34	15.56	15.06	15.25
N_*	58.35	58.43	58.62	58.37	60	56.06	56.45

Table I. Numerical values of some parameters for two choices of renormalization scale μ and different values of inflaton interaction strength κ . Each value of κ correspond to points in Figures 2 and 3 marked by numbers, which are also shown in the top rows of these tables. Smallest $|\kappa|$'s are chosen to lie at the turnover where $\mu = \phi_*$ and $\mu = \phi_{\text{end}}$ curves converge on the line joining $N_* = 50$ and $N_* = 60$ points. Largest values of $|\kappa|$ are chosen to lie on the border of 95% CL of “Planck+WP” contour in Figure 2. The ‘ h, g ’ row displays the values of the coupling constant h for $\kappa < 0$ and g for $\kappa > 0$.

of inflation only. The effect of radiative corrections on the inflationary part of the tree level potential is illustrated in Figure 1.

As Eqs. (21) - (23) cannot be solved analytically, we list out for illustrative purposes some numerical results in Table I. We also plot the results in Figure 2 together with Planck

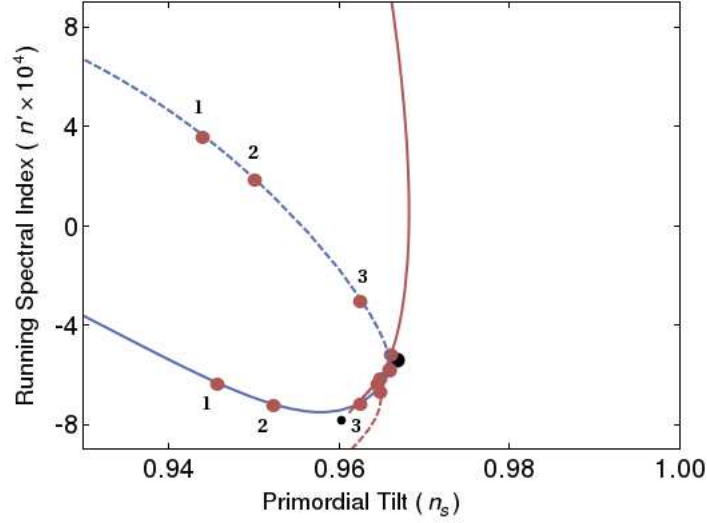


Figure 3. Plot of spectral index n_s versus spectral running n' . Numbers correspond to the same points in Figure 2 and their numerical values are given in Table I. The notation is the same as in Figure 2: black dots correspond to $\kappa = 0$ as in Ref. [6], blue curves to $\kappa < 0$ and red ones to $\kappa > 0$, solid curves correspond to $\mu = \phi_*$ and dashed ones to $\mu = \phi_{\text{end}}$.

constraints on n_s and r .

The large black dot in Fig. 2 corresponds to the “pure” $m^2\phi^2$ model with $\kappa = 0$ and $N_* = 60$, the same as in Ref. [6], while the smaller dot corresponds to $N_* = 50$. Blue curves show the effect of radiative corrections with $h \gg g$, while red curves show this effect with $g \gg h$. The solid line corresponds to the choice of the renormalization scale $\mu = \phi_*$ while the dashed line corresponds to $\mu = \phi_{\text{end}}$. Inflaton coupling to fermions, i.e. negative κ , flattens the potential, resulting in a smaller value of r as compared to the “pure” $m^2\phi^2$ case. In contrast, a coupling to bosons tends to steepen the potential, and thus increases the value of r . For a very small coupling constant, radiative corrections have negligible effect on the curvature of the potential. However, the number of efolds N_* decreases substantially. This can be seen in Figure 2 as convergence of all the four curves on the joining line from $N_* = 60$ point as they move upwards and towards the $N_* = 50$ point.

As one can see in Figure 2, different renormalization scales result in different predictions for the CMB observables if inflaton interactions are of the order of $g, h \sim 10^{-3}$. The gap between the blue solid and dashed curves in Figure 2 is of the order $\Delta r \sim 10^{-2}$, which is well within the sensitivity of future missions such as CMBpol [10] which has a planned precision

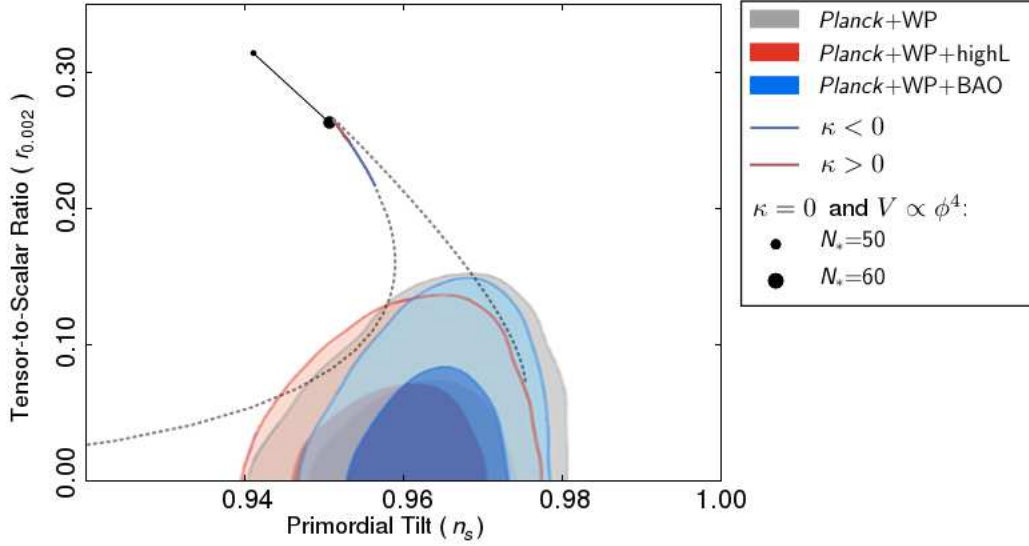


Figure 4. Planck constraints on the spectral index n_s and the tensor-to-scalar ratio r [6]. Black dots correspond to the ϕ^4 model with $\kappa = 0$. The blue curve correspond to the dominant decay channel $\phi \rightarrow \psi\bar{\psi}$ ($\kappa < 0$) and the red one to $\phi \rightarrow \chi\chi$ ($\kappa > 0$). Solid curves show the effect of one loop radiative corrections, which are subdominant to the tree level part of the potential, while gray dotted curves show the effect of large $|\kappa|$ values, such that radiative corrections dominate at least some of the inflationary part of the potential.

of the same order, or PRISM [11], which is expected to reach the precision of $\Delta r \sim 10^{-4}$.

We also plot the effect of radiative corrections on the running of the spectral index n' in Figure 3. As one can see, the difference in n' between two renormalization schemes is of the order of 10^{-4} . Measurements with such a precision will certainly be a major challenge for future missions, which cannot be achieved by CMB observations alone; rather, one needs to probe the spectral index on a much larger range of wavelengths. Such range can be measured by combining CMB and Large Scale Structure observations, of which the 21cm experiments may offer the best prospects towards this aim. The Square Kilometer Array (SKA) [12] will be able to achieve the accuracy of a few $\times 10^{-3}$ for the spectral running, while a more futuristic experiment called Fast Fourier Transform Telescope (FFTT) [13] could push this limit down by one more order of magnitude [14, 15].

C. The Case of $n = 4$

The case of the $\lambda\phi^4$ potential is less interesting than the $m^2\phi^2$ case. For the $\lambda\phi^4$ model the spectral index n_s and the tensor-to-scalar ratio r do not depend on the choice of the renormalization scale μ so that the situation is much more straightforward. We plot n_s and r including the one loop radiative corrections in Figure 4. If we require that the radiative corrections remain smaller than the tree level, the resulting modifications are still well out of the Planck 2σ contours. If one were to extend the results into the large $|\kappa|$ region (gray dotted curves in Figure 4), where the radiative corrections would dominate at least some part of the potential, one could meet the Planck constraints. However, then one should worry about the role of the higher order corrections so that obviously such a result cannot be trusted.

IV. CONCLUSIONS

The precision with which observable inflationary parameters are measured increased substantially over the last decade, culminating in the most recent results from the Planck satellite. Indeed, the data from the Planck satellite made it possible to exclude monomial ϕ^4 and ϕ^3 models of inflation with a high degree of confidence, while ϕ^2 models are on the verge of allowed region. This, however, applies only to the tree-level potential, which neglects the effects of inflaton interactions with other fields. Such interactions are necessary in any realistic model of inflation for the inflaton to reheat the universe into radiation dominated phase. These interactions, however, modify the potential of the inflaton by introducing loop corrections. In effect, the Planck constraints apply only to toy models, and the obvious question then is, what are the constraints on (semi)realistic models?

To the lowest order the modification of the inflaton potential is a Coleman-Weinberg type correction as given in Eq. (2), which is parametrized by the renormalization scale μ . In particle physics one fixes μ by determining physical masses and coupling constants of fields from measurements of interaction amplitudes at a given energy scale. For the inflaton, however, no observation exists which would give independent determination of the potential parameters.

In this work we show how different choices of the renormalization scale lead to different

predictions for observable inflationary parameters. We ignore corrections induced by the curvature and treat the inflaton itself as a classical background field. We believe that such an approach, although not completely without problems, will serve as a useful illustration of the role of radiative corrections in modifying the naive observational model constraints.

To give quantitative results we consider monomial chaotic type inflaton potentials. Radiative corrections change the slope and curvature of tree level potential, which in turn affects the predicted values of the spectral index n_s , its running n' and tensor-to-scalar ratio r . The effect of different choices of renormalization scale μ is demonstrated by choosing $\mu = \phi_*$ and $\mu = \phi_{\text{end}}$, where ϕ_* and ϕ_{end} are inflaton values when the pivot scale exits the horizon and at the end of inflation respectively. The results for the quadratic ϕ^2 potential are summarized in Figure 2 and some numerical parameter values are given in Table I. Since the renormalization scale is free, we end up with a family of models, each having a slightly different slope of the potential, which could in principle be further constrained by e.g. measuring the running of the spectral index. Meanwhile, we can conclude that within the family of semirealistic chaotic ϕ^2 models, some may be ruled out by Planck whereas some, and in particular those in which the inflaton decays predominantly into fermions, remain perfectly viable.

ACKNOWLEDGEMENTS

KE is supported by the Academy of Finland grant 1218322; MK is supported by the Academy of Finland grant 1263714.

-
- [1] E. Elizalde, S. D. Odintsov, and A. Romeo, *Improved effective potential in curved space-time and quantum matter, higher derivative gravity theory*, *Phys.Rev.* **D51** (1995) 1680–1691, [[hep-th/9410113](#)].
 - [2] M. Herranen, T. Markkanen, and A. Tranberg, *Quantum corrections to scalar field dynamics in a slow-roll space-time*, [arXiv:1311.5532](#).
 - [3] V. N. Senoguz and Q. Shafi, *Chaotic inflation, radiative corrections and precision cosmology*, *Phys.Lett.* **B668** (2008) 6–10, [[arXiv:0806.2798](#)].

- [4] D. Lyth and A. Liddle, *The Primordial Density Perturbation: Cosmology, Inflation and the Origin of Structure*. Cambridge University Press, 2009.
- [5] **Planck** Collaboration, P. Ade et al., *Planck 2013 results. XVI. Cosmological parameters*, [arXiv:1303.5076](#).
- [6] **Planck** Collaboration, P. Ade et al., *Planck 2013 results. XXII. Constraints on inflation*, [arXiv:1303.5082](#).
- [7] L. Knox and Y.-S. Song, *A limit on the detectability of the energy scale of inflation*, *Phys.Rev.Lett.* **89** (2002) 011303, [[astro-ph/0202286](#)].
- [8] A. R. Liddle and S. M. Leach, *How long before the end of inflation were observable perturbations produced?*, *Phys.Rev.* **D68** (2003) 103503, [[astro-ph/0305263](#)].
- [9] L. Kofman, A. Linde, and A. A. Starobinsky, *Towards the theory of reheating after inflation*, *Phys. Rev.* **D56** (Sep, 1997) 3258–3295, [[hep-ph/9704452](#)].
- [10] **CMBPol Study Team** Collaboration, D. Baumann et al., *CMBPol mission concept study: Probing inflation with CMB polarization*, *AIP Conf.Proc.* **1141** (2009) 10–120, [[arXiv:0811.3919](#)].
- [11] **PRISM** Collaboration, P. Andre et al., *PRISM (Polarized Radiation Imaging and Spectroscopy Mission): A White Paper on the Ultimate Polarimetric Spectro-Imaging of the Microwave and Far-Infrared Sky*, [arXiv:1306.2259](#).
- [12] “SKA project homepage at <http://www.skatelescope.org/>.”
- [13] M. Tegmark and M. Zaldarriaga, *The Fast Fourier Transform Telescope*, *Phys.Rev.* **D79** (2009) 083530, [[arXiv:0805.4414](#)].
- [14] V. Barger, Y. Gao, Y. Mao, and D. Marfatia, *Inflationary potential from 21 cm tomography and Planck*, *Phys.Lett.* **B673** (2009) 173–178, [[arXiv:0810.3337](#)].
- [15] P. Adshead, R. Easther, J. Pritchard, and A. Loeb, *Inflation and the scale dependent spectral index: Prospects and strategies*, *JCAP* **1102** (2011) 021, [[arXiv:1007.3748](#)].